A Novel on understanding How IRIS Recognition works

Vijay Shinde
Dept. of Comp. Science
M.P.M. College, Bhopal, India

Prof. Prakash Tanwar
Asst. Professor CSE
M.P.M. College, Bhopal, India

Abstract- Algorithms developed by the author for recognizing persons by their iris patterns have now been tested in six field and laboratory trials, producing no false matches in several million comparison tests. The recognition principle is the failure of a test of statistical independence on iris phase structure encoded by multi-scale quadrature wavelets. The combinatorial complexity of this phase information across different persons spans about 249 degrees of freedom and generates a discrimination entropy of about 3.2 bits/mm2 over the iris, enabling real-time decisions about personal identity with extremely high confidence. The high confidence levels are important because they allow very large databases to be searched exhaustively (one-to-many .identification mode.) without making false matches, despite so many chances. Biometrics that lack this property can only survive one-to-one (.verification.) or few comparisons. This paper explains the iris recognition algorithms, and presents results of 9.1 million comparisons among eye images from trials in Britain, the USA, Japan, and Korea.

Keywords*: *Biometric identification, Iris recognition, Hamming Distance.

I. INTRODUCTION

Biometrics technology using advanced computer techniques is now widely adopted as a front-line security measure for both identity verification and crime detection, and also offers an effective crime deterrent. Biometric techniques are used for the purpose of identifying individual by using unique characteristics of each person deterrent. A term derived from ancient Greek: 'bios' meaning 'life' and 'metric', 'to measure'. A biometric system can operate in two modes. One is Verification (authentication) which refers to the problem of confirming or denying a person's claimed identity (Am I who I claim I am?). Second is Identification (Who am I?) which refers to the problem of establishing a subject's identity - either from a set of already known identities (closed identification problem) or otherwise (open identification problem).

The human iris (Figure 1) is rich in features which can be used to quantitatively and positively distinguish one eye from another. The iris contains many collagenous fibers, contraction furrows, coronas, crypts, color, serpentine vasculature, striations, freckles, rifts, and pits. Measuring the patterns of these features and their spatial relationships to each other provides other quantifiable parameters useful to the identification process. In practical terms, statistical analyses indicate that the Iridium Technologies IRT process uses 240 degrees-of-freedom (DOF), or independent measures of variation to distinguish one iris from another.

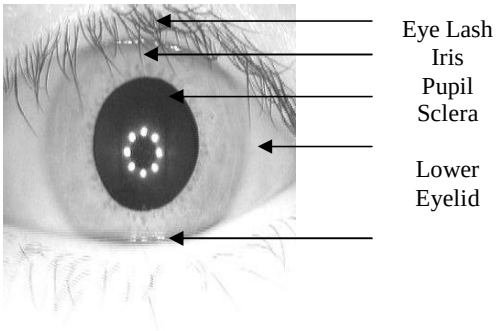

Figure 1 Typical Human Eye Image

Reliable automatic recognition of persons has long been an attractive goal. As in all pattern recognition problems, the key issue is the relation between interclass and intra-class variability: objects can be reliably classified only if the variability among different instances of a given class is less than the variability between different classes. For example in face recognition, difficulties arise from the fact that the face is a changeable social organ displaying a variety of expressions, as well as being an active 3D object whose image varies with viewing angle, pose, illumination, accoutrements, and age. It has been shown that for facial images taken at least one year apart, even the best current algorithms have error rates of 43% (Phillips et al. 2000) to 50% (Pentland et al. 2000). Against this intra-class (same face) variability, inter-class variability is limited because different faces possess the same basic set of features, in the same canonical geometry

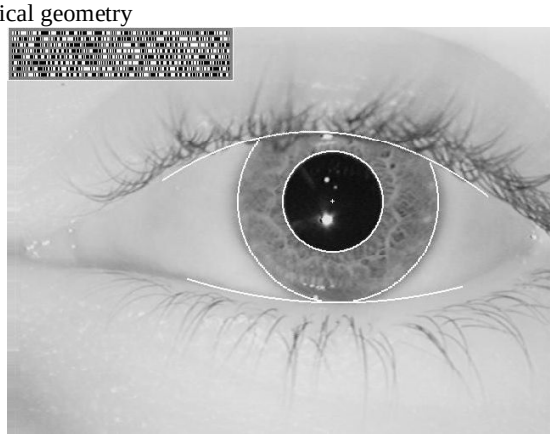

Figure 2: Example of an iris pattern, imaged monochromatically at a distance of about 35 cm. The outline overlay shows results of the iris and pupil localization and eyelid detection steps. The bit stream in the top left is the result of demodulation with complex-valued 2D Gabor wavelets to encode the phase sequence of the iris pattern

For all of these reasons, iris patterns become interesting as an alternative approach to reliable visual recognition of persons when imaging can be done at distances of less than a meter, and especially when there is a need to search very large databases without incurring any false matches despite a huge number of possibilities. Although small (11 mm) and sometimes problematic to image, the iris has the great mathematic advantage that its pattern variability among different persons is enormous. In addition, as an internal (yet externally visible) organ of the eye, the iris is well protected from the environment and stable over time. As a planar object its image is relatively insensitive to angle of illumination, and changes in viewing angle cause only affine transformations; even the no affine pattern distortion caused by pupillary dilation is readily reversible. Finally, the ease of localizing eyes in faces, and the distinctive annular shape of the iris, facilitates reliable and precise isolation of this feature and the creation of a size-invariant representation.

II. FINDING AN IRIS IN AN IMAGE

To capture the rich details of iris patterns, an imaging system should resolve a minimum of 70 pixels in iris radius. In the field trials to date, a resolved iris radius of 100 to 140 pixels has been more typical. Monochrome CCD cameras (480 x 640) have been used because NIR illumination in the 700nm - 900nm band was required for imaging to be invisible to humans. Some imaging platforms deployed a wide angle camera for coarse localization of eyes in faces, to steer the optics of a narrow-angle pan/tilt camera that acquired higher resolution images of eyes. There exist many alternative methods for finding and tracking facial features such as the eyes, and this well researched topic will not be discussed further here. In these trials, most imaging was done without active pan/tilt camera optics, but instead exploited visual feedback via a mirror or video image to enable cooperating Subjects to position their own eyes within the field of view of a single narrow-angle camera.

Focus assessment was performed in real-time (faster than video frame rate) by measuring the total high-frequency power in the 2D Fourier spectrum of each frame, and seeking to maximize this quantity either by moving an active

lens or by providing audio feedback to Subjects to adjust their range appropriately. Images passing a minimum focus criterion were then analyzed to find the iris, with precise localization of its boundaries using a coarse-to-_ne strategy terminating
in single-pixel precision estimates of the center coordinates and radius of both the iris and the pupil. Although the results of the iris search greatly constrain the pupil search, concentricity of these boundaries cannot be assumed. Very often the pupil center is nasal, and inferior, to the iris center. Its radius can range from 0.1 to 0.8 of the iris radius. Thus, all three parameters defining the pupillary circle must be estimated separately from those of the iris. A very effective
integro differential operator for determining these
parameters is:

$$\max_{(r,x_0,y_0)} \left| G_\sigma(r) * \frac{\partial}{\partial r} \oint_{r,x_0,y_0} \frac{I(x,y)}{2\pi r} ds \right| \quad (1)$$

Where I(x; y) is an image such as Fig 1 containing an eye. The operator searches over the image domain (x; y) for the maximum in the blurred partial derivative with respect to increasing radius r, of the normalized contour integral of I(x; y) along a circular arc ds of radius r and center coordinates (x_0; y_0). The symbol * denotes convolution and G_(r) is a smoothing function such as a Gaussian of scale σ. The complete operator behaves in effect as a circular edge detector, blurred at a scale set by σ, which searches iteratively for a maximum contour integral derivative with increasing radius at successively finer scales of analysis through the three parameter space of center coordinates And radius (x_0; y_0; r) defining a path of contour integration. The operator in (1) serves to find both the pupillary boundary and the outer (limbus) boundary of the iris, although the initial search for the limbus also incorporates evidence of an interior pupil to improve its robustness since the limbic boundary itself usually has extremely soft contrast when long wavelength NIR illumination is used. Once the coarse-to-_ne iterative searches for both these boundaries have reached single pixel precision, then a similar approach to detecting curvilinear edges is used to localize both the upper and lower eyelid boundaries. The path of contour integration in (1) is changed from circular to arcuate, with spline parameters fitted by standard statistical estimation methods to describe optimally the available evidence for each eyelid boundary. The result of all these localization operations is the isolation of iris tissue from other image regions, as illustrated in Fig 1 by the graphical overlay on the eye.

III. IRIS FEATURE ENCODING BY 2D WAVELET DEMODULATION

Each isolated iris pattern is then demodulated to extract its phase information using quadrature 2D Gabor wavelets (Daugman 1985, 1988, 1994). This encoding process is illustrated in Fig 2. It amounts to a patch-wise phase quantization of the iris pattern, by identifying in which quadrant of the complex plane each resultant phasor lies when a given area of the iris is projected onto complex-valued 2D Gabor wavelets:

$$h_{\{Re,Im\}} = \mathrm{sgn}_{\{Re,Im\}} \int_\rho \int_\phi I(\rho,\phi) e^{-i\omega(\theta_0-\phi)} \cdot e^{-(r_0-\rho)^2/\alpha^2} e^{-(\theta_0-\phi)^2/\beta^2} \rho d\rho d\phi \quad (2)$$

where h{Re;Im} can be regarded as a complex-valued bit whose real and imaginary parts are either 1 or 0 (sgn) depending on the sign of the 2D integral; (ρ,φ) is the raw iris image in a dimensionless polar coordinate system that is size- and translation-invariant, and which also corrects for pupil dilation as explained in a later section; α and β are the multi-scale 2D wavelet size parameters, spanning an 8-fold range from 0.15mm to 1.2mm on the iris; ώ is wavelet frequency, spanning 3 octaves in inverse proportion to β; and (r0; θ0) represent the polar coordinates of each region of iris for which the phase or coordinates h{Re;Im} are computed. Such a phase quadrant coding sequence is illustrated for one iris by the bit stream shown graphically in Fig 1. A desirable feature of the phase code portrayed in Fig 2 is that it is a cyclic, or grey code: in rotating between any adjacent phase quadrants, only a single bit changes, unlike a binary code in which two bits may change, making some errors arbitrarily more costly than others. Altogether 2,048 such phase bits (256 bytes) are computed for each iris, but in a major improvement over the earlier (Daugman 1993) algorithms, now an equal number of masking bits are also computed to signify whether any

iris region is obscured by eyelids, contains any eyelash occlusions, specular reflections, boundary artifacts of hard contact lenses, or poor signal-to-noise ratio and thus should be ignored in the demodulation code as artifact.

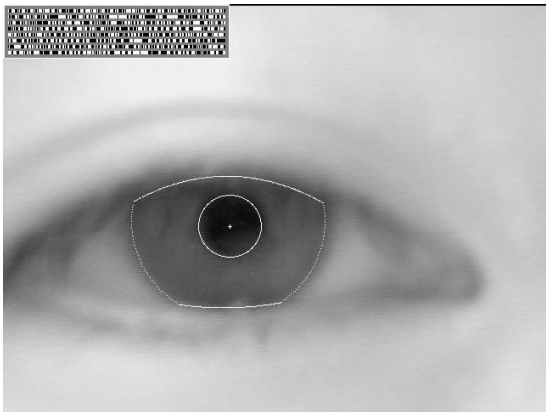

Figure 3: Illustration that even for poorly focused eye images, the bits of a demodulation phase sequence are still set, primarily by random CCD noise. This prevents poorly focused eye images from resembling each other in the pattern matching stage, in the way that (e.g.) poorly resolved face images look alike and can be confused with each other.

Only phase information is used for recognizing irises because amplitude information is not very dis-criminating, and it depends upon extraneous factors such as imaging contrast, illumination, and camera gain. The phase bit settings which code the sequence of projection quadrants as shown in Fig 2 capture the information of wavelet zero-crossings, as is clear from the sign operator in (2). The extraction of phase has the further advantage that phase angles are as-signed regardless of how low the image contrast may be, as illustrated by the extremely out-of-focus image in Fig 3. Its phase bit stream has statistical proper-ties such as run lengths similar to those of the code for the properly focused eye image in Fig 1. (Fig 3 also illustrates the robustness of the iris- and pupil finding operators, and the eyelid detection operators, despite poor focus.) The benefit which arises from the fact that phase bits are set also for a poorly focused image as shown here, even if based only on random CCD noise, is that different poorly focused irises never become confused with each other when their phase codes are compared. By contrast, images of different faces look increasingly alike when poorly resolved, and may be confused with each other by appearance-based face recognition algorithms.

IV. RECOGNIZING IRISES REGARDLESS OF SIZE, POSITION, AND ORIENTATION

Robust representations for pattern recognition must be invariant to changes in the size, position, and orientation of the patterns. In the case of iris recognition, this means we must create a representation that is invariant to the optical size of the iris in the image (which depends upon the distance to the eye, and the camera optical magnification factor); the size of the pupil within the iris (which introduces a non-fine pattern deformation); the location of the iris within the image; and the iris orientation, which depends upon head tilt, torsional eye rotation within its socket (cyclovergence), and camera angles, com-pounded with imaging through pan/tilt eye- finding mirrors that introduce additional image rotation factors as a function of eye position, camera position, and mirror angles. Fortunately, invariance to all of these factors can readily be achieved.

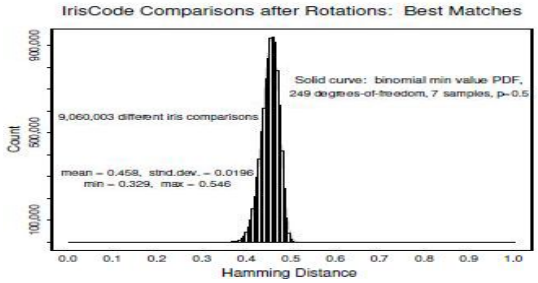

Figure 4: Distribution of Hamming Distances from the same set of 9.1 million comparisons

V. UNIQUENESS OF FAILING THE TEST OF STATISTICAL INDEPENDENCE

The statistical data and theory presented above show that we can perform iris recognition success-fully just by a test of statistical independence. Any two different irises are statistically "guaranteed" to pass this test of independence, and any two images that fail this test (i.e. produce a HD 0.32) must be images of the same iris. Thus, it is the unique failure of the test of independence, that is the basis for iris recognition.

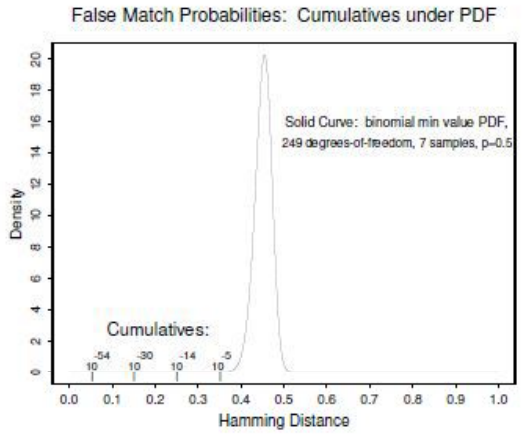

Figure 5: Calculated cumulative under the left tail of the distribution seen in Fig 4.

It is informative to calculate the significance of any observed HD matching score, in terms of the likelihood that it could have arisen by chance from two different irises. These probabilities give a confidence level associated with any recognition decision. Fig 5 shows the false match probabilities marked off in cumulative along the tail of the distribution presented in Fig 4. Table 1 enumerates the cumulative of (11) (false match probabilities) as a more fine-grained function of HD decision criterion in the range between 0.26 and 0.35. Calculation of the large factorial terms in (4) was done with Stirling's approximation which errs by less than 1% for n >= 9

HD Criterion	**Odds of False Match**
0.26	1 in 10^{13}
0.27	1 in 10^{12}
0.28	1 in 10^{11}
0.29	1 in 13 billion
0.30	1 in 1.5 billion
0.31	1 in 185 million
0.32	1 in 26 million
0.33	1 in 4 million
0.34	1 in 690,000
0.35	1 in 133,000

:

Table 1: Cumulative under giving single false match probabilities for various HD criteria.

The algorithms for iris recognition exploit the extremely rapid attenuation of the HD distribution tail created by binomial combinatory, to accommodate very large database searches without suffering false matches. The HD threshold is adaptive, to maintain PN < 10^6 regardless of how large the search database size N is.

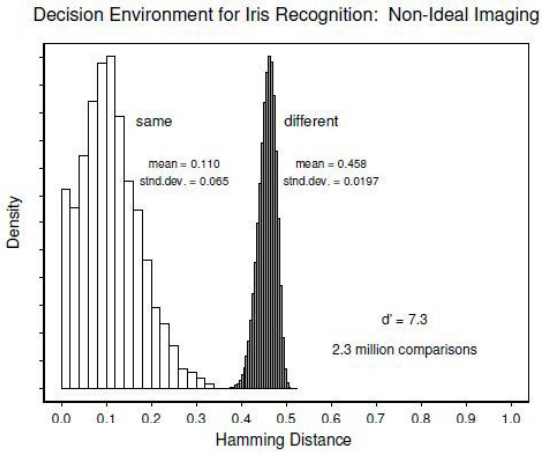

Figure 6: The Decision Environment for iris recognition under relatively unfavorable conditions, using images acquired at different distances, and by different optical platforms.

As Table 1 illustrates, this means that if the search database contains 1 million different iris patterns, it is only necessary for the HD match criterion to adjust downwards from 0.33 to 0.27 in order to maintain still a net false match probability of 10^6 for the entire database.

VI. DECISION ENVIRONMENTS FOR IRIS RECOGNITION

The overall decidability. of the task of recognizing persons by their iris patterns is revealed by comparing the Hamming Distance distributions for same versus for different irises. The left distribution in Fig 6 shows the HDs computed between 7,070 different pairs of same-eye images at different times, under different conditions, and usually with different cameras; and the right distribution gives the same 9.1 million comparisons among different eyes shown earlier. To the degree that one can confidently decide whether an observed sample belongs to the left or the right distribution in Fig 6, iris recognition can be successfully performed. Such a dual distribution representation of the decision problem may be called the .decision environment, because it reveals the extent to which the two cases (same versus different) are separable and thus how reliably decisions can be made, since the overlap between the two distributions determines the error rates. Whereas Fig 6 shows the decision environment under less favorable conditions (images acquired by different camera platforms), Fig 7 shows the decision environment under ideal (almost artificial) conditions. Subjects' eyes were imaged in a laboratory setting using always the same camera with fixed zoom factor and at fixed distance, and with fixed illumination Not surprisingly, more than half of such image comparisons achieved an HD of 0.00, and the average HD was a mere 0.019. It is clear from comparing Fig 6 and Fig 7 that the .authentic. Distribution for iris recognition (the similarity between different images of the same eye, as shown in the left-side distributions), depends very strongly upon the image acquisition conditions. However, the measured similarity for .imposters. (the right-side distribution) is apparently almost completely independent of imaging factors. Instead, it mainly reflects just the combinatory of Bernoulli trials, as bits from independent binary sources (the phase codes for different irises) are compared.

VII. SPEED PERFORMANCE SUMMARY

On a 300 MHz Sun workstation, the execution times for the critical steps in iris recognition are as follows, using optimized integer code:

Operation	Time
Assess image focus	15 msec
Scrub specular reflections	56 msec
Localize eye and iris	90 msec
Fit pupillary boundary	12 msec
Detect and fit both eyelids	93 msec
Remove lashes and contact lens edges	78 msec
Demodulation and Iris Code creation	102 msec
XOR comparison of two Iris Codes	10 μs

Table 2: Speeds of various stages in the iris recognition process.

The search engine can perform about 100,000 full comparisons between different irises per second, because of the efficient implementation of the matching process in terms of elementary Boolean operators EX-OR and ∩ acting in parallel on the computed phase bit sequences. If database size was measured in millions of enrolled persons, then the inherent parallelism of the search process should be exploited for the sake of speed by dividing up the entire search database into units of about 100,000 persons each. The confidence levels shown in Table 1 indicate how the decision threshold should be adapted for each of these parallel search engines, in order to ensure that no false matches were made despite several large-scale searches being conducted independently. The mathematics of the iris recognition algorithms make it clear that databases the size of entire nations could be searched in parallel to make a confident identification decision, in about 1 second using parallel banks of inexpensive CPUs, if such large national iris databases ever came to exist.

REFERENCES

[1] Adini, Y., Moses, Y., and Ullman, S. (1997) Face recognition: the problem of compensating for changes in illumination direction. *Trans. Pat. Anal. Mach. Intell.* 19(7): 721-732.

[2] Belhumeur, P.N., Hespanha, J.P., and Kriegman, D.J. (1997) Eigenfaces vs. Fisherfaces: Recognition using class-speci c linear projection. *Trans. Pat. Anal. Mach. Intell.* 19(7): 711-720.

[3] Berggren, L. (1985) Iridology: A critical re-view. *Acta Ophthalmologica* 63(1): 1-8.

[4] Chedekel, M.R. (1995) Photophysics and photo-chemistry of melanin. In: *Melanin: Its Role in Human Photoprotection.* Valdenmar: Overland Park, 11-23.

[5] Cover, T. and Thomas, J. (1991) *Elements of Information Theory*. Wiley: New York.

[6] Daugman, J. (1985) Uncertainty relation for resolution in space, spatial frequency, and orientation optimized by two-dimensional visual cortical lters. *Journal of the Optical Society of America A* 2(7): 1160-1169.

[7] Daugman, J. (1988) Complete discrete 2D Ga-bor transforms by neural networks for image analysis and compression. *Trans. Acous. Sp. Sig. Proc.* 36(7): 1169-1179.

[8] Daugman, J. (1993) High con dence visual recogni-tion of persons by a test of statistical independence. *Trans. Pattern Analysis and Machine Intelligence* 15(11): 1148-1161.

[9] Daugman, J. (1994) U.S. Patent No. 5,291,560: *Biometric Personal Identi cation System Based on Iris Analysis.* Issue Date: 1 March 1994.

[10] Daugman J. (2001) Statistical richness of visual phase information: Update on recognizing persons by their iris patterns. *International Journal of Computer Vision* 45(1): 25-38.

[11] Daugman, J., and Downing, C. (1995) Demodu-lation, predictive coding, and spatial vision. *Journal of the Optical Society of America A* 12(4): 641-660.

[12] Daugman, J., and Downing, C. (2001) Epige-netic randomness, complexity, and singularity of human iris patterns. *Proceedings of the Royal Society, Biological Sciences* 268: 1737-1740.

[13] Kronfeld, P. (1962) Gross anatomy and embry-ology of the eye. In: *The Eye* (H. Davson, Ed.) Academic Press: London.

[14] Pentland, A., and Choudhury, T. (2000) Face recognition for smart environments. *Computer* 33(2): 50-55.

[15] Phillips, P.J., Martin, A., Wilson, C.L., and Przy-bocki, M. (2000) An introduction to evaluating biometric systems. *Computer* 33(2): 56-63.

[16] Phillips, P.J., Moon, H., Rizvi, S.A., and Rauss, P.J. (2000) The FERET evaluation methodology for face-recognition algorithms. *Trans. Pat. Anal. Mach. Intell.* 22(10): 1090-1104.

[17] Simon, A., Worthen, D.M., and Mitas, J.A. (1979) An evaluation of iridology. *Journal of the American Medical Association* 242: 1385-1387.

[18] Viveros, R., Balasubramanian, K., and Balakr-ishnan, N. (1984) Binomial and negative binomial analogues under correlated Bernoulli trials. *The American Statistician* 48(3): 243-247.